Functionalized Graphene



Tailoring Surface Properties via Functionalized Hydrofluorinated Graphene Compounds

Jangyup Son, Nikita Buzov, Sihan Chen, Dongchul Sung, Huije Ryu, Junyoung Kwon, SunPhil Kim, Shunya Namiki, Jingwei Xu, Suklyun Hong, Kenji Watanabe, Takashi Taniguchi, William P. King, Gwan-Hyoung Lee, and Arend M. van der Zande*

A new compound material of 2D hydrofluorinated graphene (HFG) is demonstrated whose relative hydrogen/fluorine concentrations can be tailored between the extremes of either hydrogenated graphene (HG) and fluorinated graphene (FG). The material is fabricated through subsequent exposures to indirect hydrogen plasma and xenon difluoride (XeF₂). Controlling the relative concentration in the HFG compound enables tailoring of material properties between the extremes offered by the constituent materials and in-plane patterning produces micrometer-scale regions with different surface properties. The utility of the technique to tailor the surface wettability, surface friction, and electrical conductivity is demonstrated. HFG compounds display wettability between the extremes of pure FG with contact angle of $95^{\circ} \pm 5^{\circ}$ and pure HG with contact angle of $42^{\circ} \pm 2^{\circ}$. Similarly, the HFG surface friction may be tailored between the two extremes. Finally, the HFG electrical conductivity tunes through five orders of magnitude when transitioning from FG to HG. When combined with simulation, the electrical measurements reveal the mechanism producing the compound to be a dynamic process of adatom desorption and replacement. This study opens a new class of 2D compound materials and innovative chemical patterning with applications for atomically thin 2D circuits consisting of chemically/ electrically modulated regions.

An important question at the forefront of 2D materials research is how many different kinds of 2D materials can exist and what are the ranges of properties that may be accessed and tailored. In particular, while there are known to be more than a thousand separate members of the family

of 2D materials,^[1] the number expands dramatically when considering compounds. In graphene, transition metal dichalcogenides (TMDCs), and hexagonal boron nitride (hBN), compounding and alloying through altering chemical composition^[2] or substitution with heteroatoms,[3,4] and additive intercalation[5] is already an important strategy for tailoring the electronic, optical, and mechanical properties. Examples include doping and tailoring the bandgap in ternary 2D alloys, [6,7] and phase change materials in $W_x Mo_{1-x} Te_2$ alloys.^[8] However, these strategies often become challenging in the monolayer limit where substitutional doping often leads to undesired out-ofplane defects and unstable phases with loss of advantageous properties.^[9] An alternate and highly successful strategy available to monolayer 2D materials is chemical functionalization of the van der Waals (vdW) surface.[10-13] For example, exposing graphene to xenon difluoride (XeF_2) gas^[14–16] or low energy hydrogen (H) plasma,[17,18] respectively, leads to

fluorinated graphene (FG) or hydrogenated graphene (HG) wherein the chemisorption of foreign atoms transforms the carbon bonds from semimetallic sp² hybridization into insulating sp³ hybridization.^[17,18] HG and FG are chemically distinct with very different surface properties.^[19] A novel question is whether it is possible to generate mixed compounds

Dr. J. Son, N. Buzov, [+] S. Chen, S. P. Kim, S. Namiki, J. Xu, Prof. W. P. King, Prof. A. M. van der Zande
Department of Mechanical Science and Engineering
University of Illinois Urbana-Champaign
Urbana 61801, IL, USA
E-mail: arendv@illinois.edu
Dr. J. Son, H. Ryu, Prof. G.-H. Lee
Department of Material Science and Engineering
Seoul National University
Seoul 08826, Korea

The ORCID identification number(s) for the author(s) of this article can be found under https://doi.org/10.1002/adma.201903424.

[+]Present address: Electrical and Computer Engineering Department, University of California, Santa Barbara, Santa Barbara 93106, CA, USA Dr. D. Sung, Prof. S. Hong
Graphene Research Institute
Department of Physics and Astronomy, and Graphene Research InstituteTexas Photonics Center International Research Center (GRI-TPC IRC)
Sejong University
Seoul 05006, Korea
J. Kwon
Department of Materials Science and Engineering
Yonsei University

Dr. K. Watanabe, Dr. T. Taniguchi National Institute for Materials Science Namiki, Tsukuba 305-0044, Ibaraki, Japan

Seoul 03722, Korea

DOI: 10.1002/adma.201903424

ADVANCED MATERIALS

www.advmat.de

from HG and FG to tailor the properties in the same fashion as substitutional doping. Creating a compound material from a mixture of HG and FG will open up a new class of synthetic 2D materials that have not yet been explored and a new strategy for engineering the properties in the monolayer limit.

Two recent papers have demonstrated the possibility of creating mixed hydrogenated fluorographene in solution. [20,21] However, as liquid dispersions, it is not possible to explore the impact of the compound mixture on the surface properties of the graphene, nor apply any of the patterning techniques which would enable the integration of this new material into devices. Surface chemical functionalization has several advantages over solution processing. First, it may be performed after synthesis while the graphene is on the target substrate. Second, in 2D materials, there is no distinction between the surface and the bulk, so functionalization enables tailoring not just the electronic properties[17,22] but also surface characteristics like wettability[23-25] and molecular adhesion.[26] Third, the functionalization is reversible and amenable to nanofabrication allowing patterning via conventional lithography or tip-based nanofabrication like heating or friction.[27] Bringing these capabilities together, the combination of patterning and tailoring compound 2D materials are critical to creating 2D integrated systems^[28,29] such as atomically thin electronic circuits, [30] lab-on-a-chip (LOC), [31] and chemically patterned nanotemplates [32] for future transparent, wearable, flexible, and stretchable technologies.

In this work, we present a novel method for creating, patterning, and tailoring the surface properties of a new compound functionalized hydrofluorinated graphene made by sequential exposure of graphene to low energy H plasma and XeF₂ gas. We demonstrate reversible switching of the surface between completely HG and FG as well as the intermediate relative concentration of hydrogen to fluorine. This result is novel, as it was unknown whether already functionalized materials would interact or generate stable states when exposed to a new functionalization agent. By masking the surface during exposure, we demonstrate patterning of four chemically distinct materials on a single surface-graphene, FG, HG, and hydrofluorinated graphene. These patterned structures enable direct comparisons of the relative surface properties such as wettability and friction and show that controlling the relative adatom concentration modulates the surface properties. The hydrofluorinated graphene showed intermediate surface characteristics such as the wetting angle between $95^{\circ} \pm 5^{\circ}$ of hydrophobic FG to $42^{\circ} \pm 2^{\circ}$ of hydrophilic HG. Additionally, the relative surface friction can be tailored to be in an intermediate state between FG and HG. Surprisingly, the electrical properties of functionalized graphene showed unusual recovery of electrical conductance during partial transformation of FG to hydrofluorinated graphene. We use simulations to show that this recovery is a result of the dynamics of the changeover in chemical species wherein initially F adatoms are removed from the FG surface when exposed to foreign H adatoms, and then the H atoms bind to the newly opened graphene sites.

Figure 1a shows a schematic of the synthesis process for generating hydrofluorinated graphene compound through sequential fluorination and hydrogenation. First, graphene on silicon dioxide substrate was exposed to XeF_2 gas to generate $FG^{[14-16]}$ or indirect H plasma to generate HG.^[17] These materials are known to form a one-sided functionalization of the top surface with a structure

of C_4X (X = F or H).^[16,17,33,34] Our innovation is to conduct an additional functionalization step by exposing the already functionalized FG/HG to the other source of H plasma/XeF₂, respectively. The sequential exposure generates a new functionalized hydrofluorinated graphene, where the amount of F and H on the graphene surface depends on the relative exposure times to the two sources. The details of graphene transfer, cleaning, and additional functionalization parameters are available in Sections S1.1 and S1.2 in the Supporting Information. Throughout the paper, the labels of hydrofluorinated graphene are used to indicate the order of functionalization, with HFG/FHG referring to the graphene that has first been fluorinated/hydrogenated and then hydrogenated/fluorinated. These labels are not an indicator of the relative concentration of H versus F.

To confirm the chemical bonding of the hydrofluorinated graphene, we performed X-ray photoelectron spectroscopy (XPS). Figure 1b is a plot of XPS spectra of representative samples of graphene, FG, HG, and HFG. The graphene shows the sp² bond peak in C 1s core-level spectra centered at 284.5 eV. In the HG, this peak was broadened and shifted to a higher binding energy by 0.4 eV, indicating that H atoms are covalently bonded with C atoms on the graphene surface, transforming the π -bonds to C-H bonds.[17,18,33] In the FG, two peaks emerge at 287.6 and 290.8 eV, indicating formation of semi-ionic and covalent C-F bonds, respectively. [25] The coverage of H and F calculated from XPS peak areas of C 1s spectra are 23% and 27% for HG and FG, respectively, which are comparable to previous results in single-side functionalized graphene.[16,17,33,34] After hydrogenation of FG, C-F bond peaks are reduced, which means that C-F bonds are broken by H adatoms. Additional measurements with Raman spectroscopy support the change in bonding states of the functionalized graphene (Figure S1, Supporting Information).

Next, we examine the relation between exposure time and composition. Figure 1c is a plot of the change in the XPS signature for FG under increasing exposure time to H plasma. As hydrogenation time increased from 5 to 15 min, semi-ionic and covalent C–F bonds peaks decrease and disappear. After 15 min, the transformed C 1s spectrum is very similar to pure HG (Figure 1b). Similarly, Figure 1d is a plot of the change in the XPS signature for the reverse process of HG under increasing exposure to XeF₂, and show a continuous transition from HG to FG, with FHG states in between. These measurements show reversible switching between fluorination and hydrogenation of graphene and the generation and control of the relative concentration of intermediate states of HFG or FHG.

Next, we demonstrate spatial patterning of the chemical composition of graphene. Figure 2a is an optical image of graphene patterned into a cross hatch with regions of graphene, HG, FG, and HFG on the same substrate. Figure 2b is a diagram of the chemical functionalization pattern at one of the intersections between the regions (see fabrication details in Figures S2 and S3 in the Supporting Information). We confirm the spatial patterning and relative concentration of the functionalized graphene through time-of-flight secondary ion mass spectrometry (TOF-SIMS). Figure 2c,d, respectively, are the spatial concentration maps of F and H over one patterned intersection, with each region indicated. Figure 2c shows the largest F concentration in the FG region, essentially zero F in the pristine graphene and



www.advmat.de

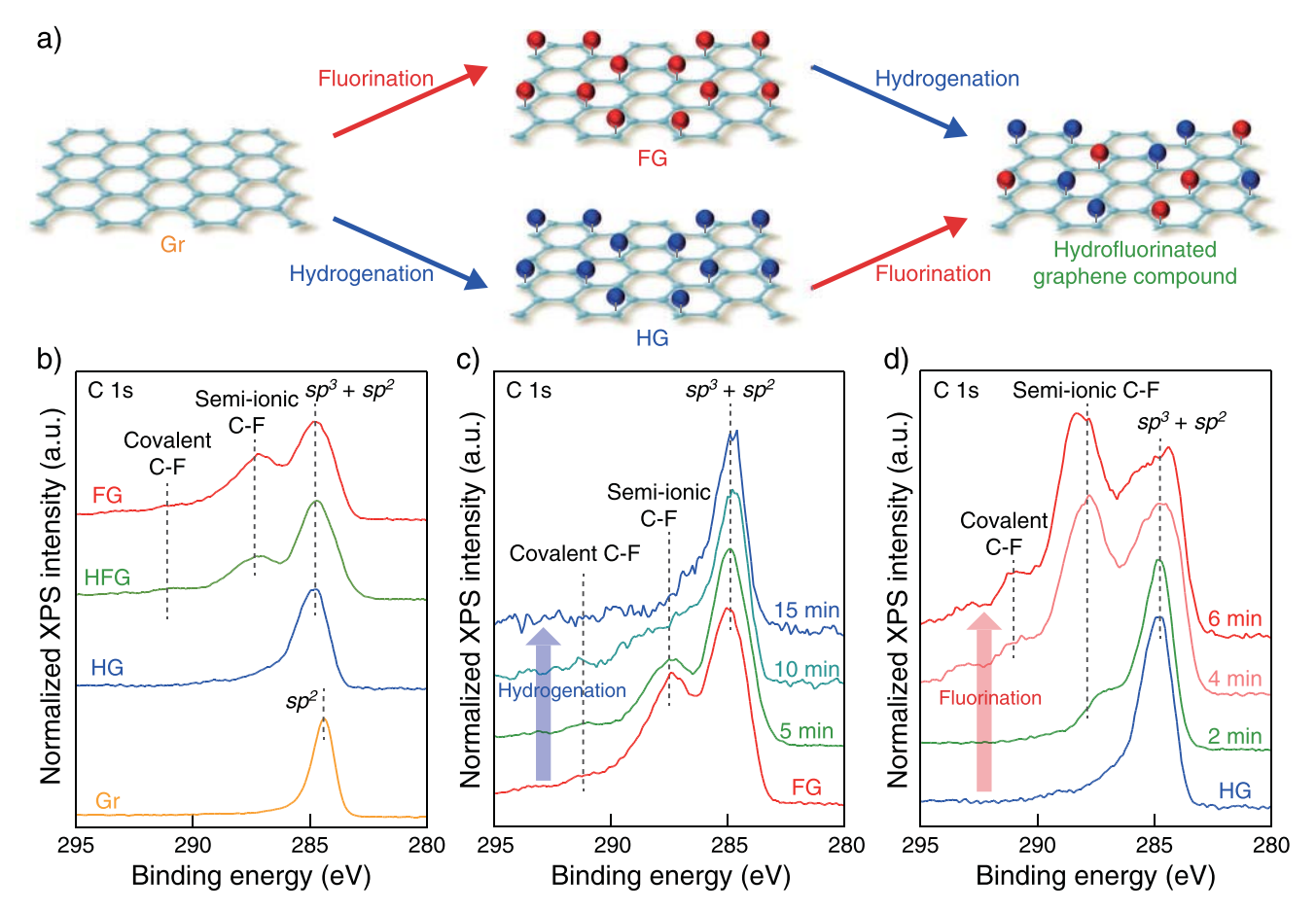


Figure 1. a) Schematic illustration of the sequential functionalization process for generating hydrofluorinated graphene. b) XPS of the C 1s core-level spectra comparing: pristine graphene, HG, HFG, and FG. c) The time evolution of C 1s spectra in FG exposed to H plasma for 0, 5, 10, and 15 min. d) The time evolution of C 1s spectra in HG exposed to XeF $_2$ gas for 0, 2, 4, and 6 min.

HG regions, and an intermediate concentration of F in the compound HFG region. Correspondingly, Figure 2d shows essentially zero H in the FG region, similar concentrations of H in the pristine graphene and HG regions, and an intermediate concentration in the HFG region. This confirms that the sequential exposure to F and H is not just adding more material, but is substituting one element for another. The similar concentration of H on the pristine graphene as the HG is due to the presence of residual hydrocarbons on the surface due to the transfer procedure (see Figure S4 in the Supporting Information). Figure 2e,f are the TOF-SIMS maps showing that sequential masking also allows the fabrication of spatially patterned concentration gradients (fabrication details in Figures S5 and S6, Supporting Information). The edges between each region are very sharp, below the resolution of the instruments of <1 µm for TOF-SIMS and < 40 nm for scanned probe measurements discussed below.

Figures 3 and **4** examine how the relative concentration of H and F tailors the surface and the electrical properties of the graphene. Figure 3a is a plot of the surface wetting angle of water droplets deposited onto pristine graphene, FG, HG, and HFG. Surface wettability has been previously reported for pristine graphene, [35,36] FG, [37] and HG, [24] but not the hydrofluorinated graphene. The wettability measurements were performed on different regions of a 4-quadrant patterned sample discussed

in Figure 2a-d (Section S1.2 and Figure S7, Supporting Information). There is some controversy about the hydrophobicity of FG in the literature.[37] Our results do not resolve this fundamental question. However, we note that our structures allow direct comparison of the variation in surface chemistry and properties on an otherwise identical sample removing experimental uncertainties like variations in fabrication, underlying substrate, [35,38,39] surface energy, [40] and measurement conditions.^[41] As shown in the insets of Figure 3a, each region exhibits a distinct wetting angle. The wetting angle for pristine graphene on SiO_2 was $82 \pm 4^{\circ}$, [35,36] showing that it is mildly hydrophilic. The error was calculated as the standard deviation from 10 independent measurements on the same droplet on each sample. The wetting angle of the FG region (fluorination 6 min) increased to 95 \pm 5°, showing a small increase in hydrophobicity. In contrast, the wetting angle of HG (hydrogenation 5 min) was $42 \pm 2^{\circ}$, showing a significant increase in hydrophilicity. Meanwhile, the wetting angle of the HFG (hydrogenation 5 min after fluorination 6 min) was an intermediate value of $60 \pm 3^{\circ}$. These results indicate that controlled chemical mixing of the compound HFG provides a knob to tune and pattern the wettability of graphene.

In Figure 3b,c, we investigate the surface friction of HFG using friction force microscopy. Figure 3b shows the map of the

www.advmat.de

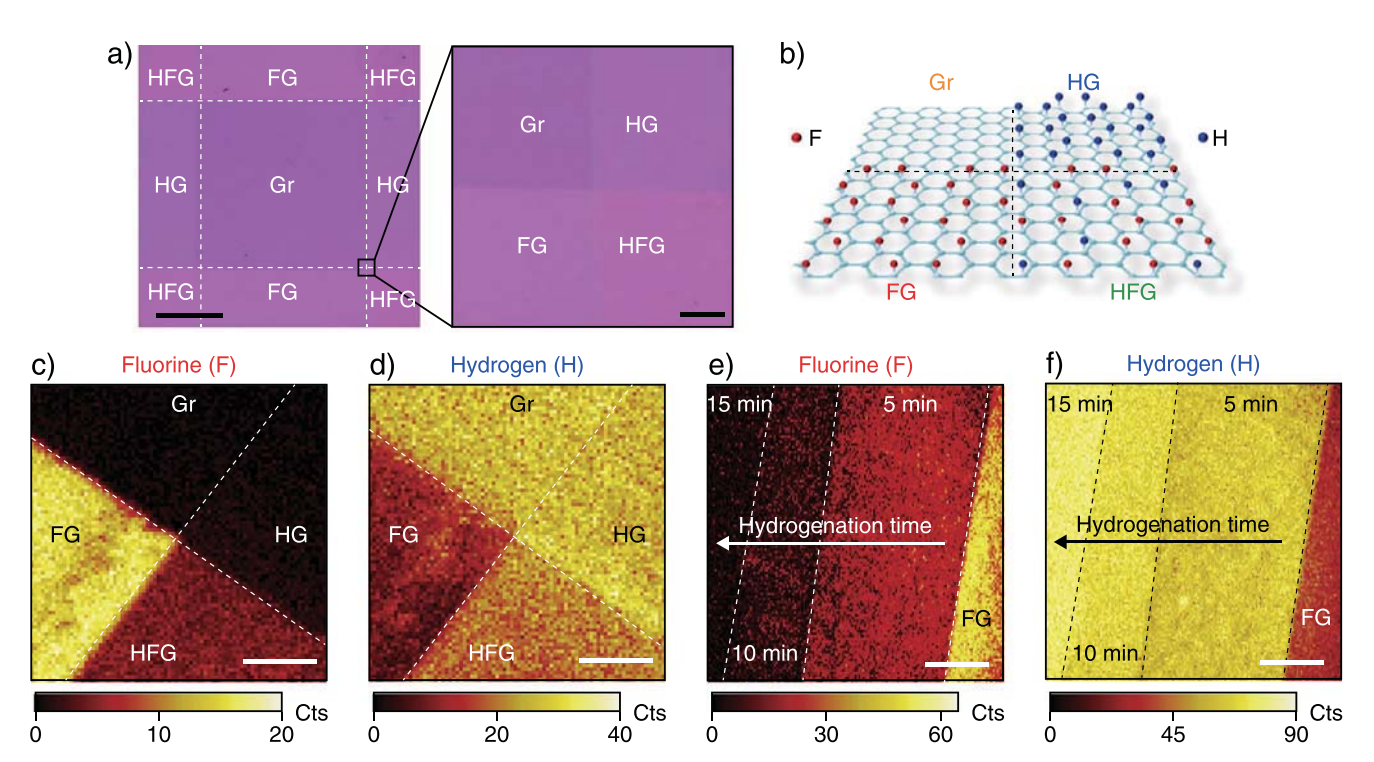


Figure 2. a) Optical images and b) schematic illustration of chemically patterned graphene areas consisting of pristine graphene, FG, HG, and HFG. Scale bars are 5 mm and 5 μ m, respectively. c,d) TOF-SIMS plots of the surface fluorine and hydrogen concentration over one chemically patterned graphene intersection (scale bars: 50 μ m). e,f) TOF-SIMS plots of surface fluorine and hydrogen concentration over a patterned surface wherein each region in FG was exposed to different hydrogenation time from 0 to 15 min.

friction signal over a 4-quadrant intersection (hydrogenation 5 min after fluorination 6 min) between different materials like the one shown in Figure 2a. Figure 3c shows line profiles of the relative surface friction across each material interface from the positions identified with white arrows in Figure 3b. Pristine graphene shows the lowest relative friction, while HG, HFG, and FG exhibit 3-, 4-, and 7-fold enhancement of the surface friction, respectively. The relative difference in the surface friction between graphene, HG, and FG is similar to previous reports. [42] Once again, HFG exhibits an intermediate value between HG and FG. Figure S8 in the Supporting

Information shows the friction of HFG with a longer second exposure (hydrogenation 20 min) is transformed into nearly that of HG.

To explain the change in friction, we note that chemical functionalization alters both the adhesion strength and the mechanical stiffness of pristine graphene, and the friction is determined in proportion to the product of these two factors. [42] Theoretical calculations predict that the increase of the mechanical stiffness dominates the enhancement of nanoscale friction over the decrease of the adhesion strength. Therefore, the functionalized graphene regions in our study show higher

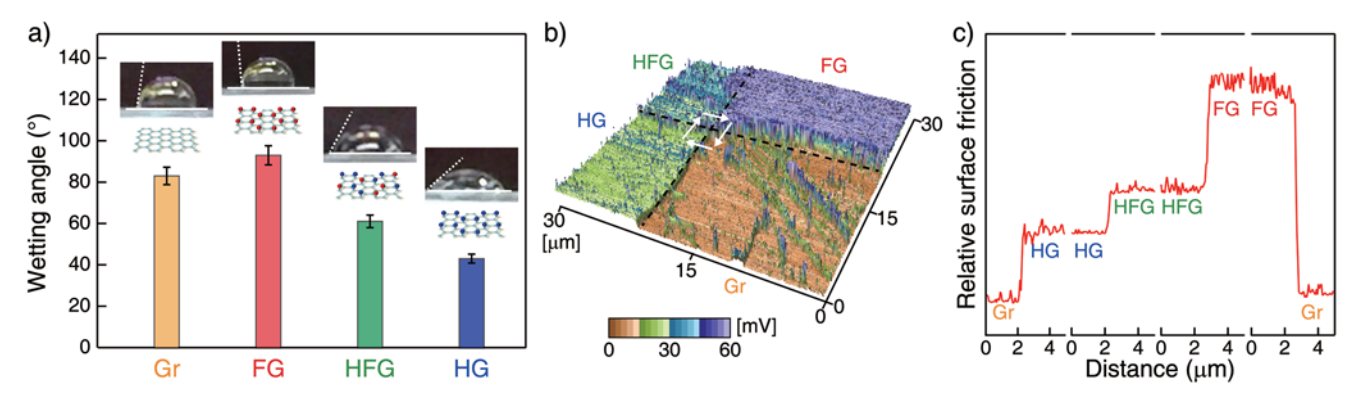


Figure 3. a) Wetting angles of water droplets on Gr, FG, HG, and HFG surfaces. Insets are images of representative droplets on each surface. b) 2D map of the relative surface friction over one intersection from Figure 2a, measured by friction force microscopy. Black dotted lines identify the boundaries between each surface. c) Line profiles of the relative surface friction measured by friction force microscopy across interfaces between regions of different functionalization, identified by the white arrows in (b). Each region showed clearly distinguishable surface friction with HG, HFG, and FG exhibiting 3-, 4-, and 7-fold enhanced relative surface friction, respectively, compared to graphene.

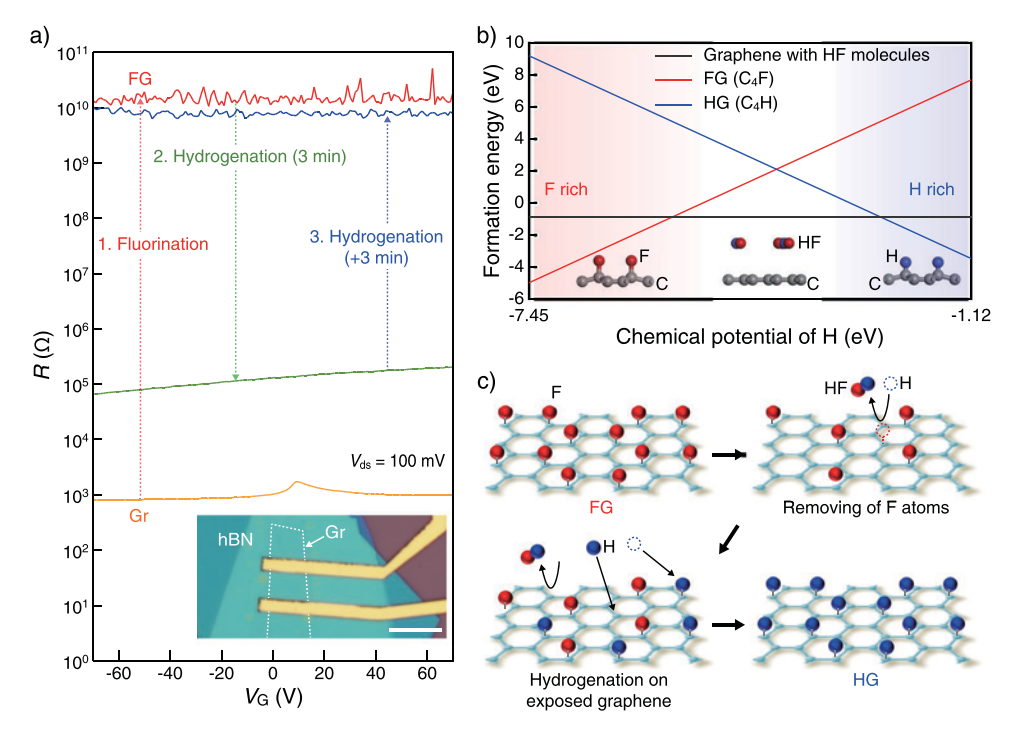


Figure 4. a) Resistance of a graphene FET on hBN under sequential functionalization of: 1) fluorination for 6 min, 2) hydrogenation for 3 min more. Inset is an optical image of the transistor before functionalization (scale bar: 5 μ m). b) Formation energies for FG, graphene with HF molecules, and HG as a function of hydrogen chemical potential μ H. The most stable structures at each formation energy are shown. The formation energy of pristine graphene is set to zero. c) A schematic illustration of the chemical reaction taking place during hydrogenating FG. Hydrogen will either bind with fluorine to form HF gas or bind to open graphene sites to form HG. The probability of these two processes occurring will change with time and the relative concentration of FG, open graphene sites, and HG.

relative surface friction than that of graphene, and its magnitude depends on the relative H/F concentration.

Next, we examine the change in electrical resistance of graphene during sequential functionalization. As shown in the inset in Figure 4a, we fabricated an hBN-encapsulated graphene field-effect transistor (FET) using established techniques (Section S1.9, Supporting Information). The hBN acts as an ideal electronic substrate to allow us to investigate the intrinsic response of the modified graphene with low hysteresis or doping.^[43,44] As we have shown previously, graphene acts as an impermeable etch mask to protect the underlying hBN during the chemical modification of the graphene.^[16]

Figure 4a is a plot of the gate-dependent resistance of the device through sequential stages of chemical functionalization from pristine graphene, to FG (fluorination 6 min), to HFG (partial hydrogenation 3 min), and finally to HG (hydrogenation for 3 more minutes). The pristine graphene showed low approximately kiloohm resistance and the expected Dirac gate behavior. After fluorination the FG resistance increased to a few gigaohms. After partial hydrogenation, the HFG resistance dramatically decreased to $\approx 100~\mathrm{k}\Omega$, five orders of magnitude smaller than the FG. However, additional hydrogenation of the same sample resulted in a return to the high resistance of approximately gigaohm, similar to the FG.

To understand the origin of the resistance changes and the dynamics of the atomic exchange, we performed density functional theory (DFT) simulations (Section S1.10 and Figure S9, Supporting Information). Figures 4b shows the formation

energies of FG, HG, and pristine graphene with HF molecules as a function of hydrogen chemical potential $\mu_{\rm H}$. Insets are the most stable structures at each chemical potential. Unsurprisingly, the FG and HG is the most stable in the F-rich and H-rich chemical potentials, respectively. Less obviously, graphene with HF molecules is the most stable structure for intermediate concentrations corresponding with chemical potentials $-5.4 < \mu_{\rm H} < -2.4$. These simulations show that free hydrogen will react with fluorine bonded to carbon to form hydrofluoric (HF) gas and will react with open graphene sites to form HG. These simulations do not account for the extra energy of the source plasma or the dynamics of the exchange.

From the conductivity measurements and the DFT simulations, we infer that the hydrogenation of FG consists of two steps, illustrated in Figure 4c. In pure FG, there are no vacant graphene sites for hydrogen to bind to, so the removal of fluorine will initially dominate. The recovered sp² bonded carbons lead to percolation paths in the graphene, and an initial decrease in resistance. Under increased exposure, the open sites are filled with hydrogen leading to a return to an insulating state. As further evidence for this interpretation, we provide Raman spectra of the graphene FET at each exposure time (Figure S10, Supporting Information), and electronic band structures (Figure S11, Supporting Information).

In summary, we have demonstrated the synthesis of a new 2D hydrofluorinated graphene compound and revealed the mechanism of the switching of the surface adatoms. The properties of the compound such as wettability, surface friction, and

ADVANCED MATERIALS

vww.advmat.de

electrical conductivity were tuned by the relative adatom concentration. In addition, we demonstrated in-plane patterning of the concentration through sequential masking during functionalization to generate gradients and discrete regions with tailored properties. These new graphene-based 2D compounds and innovative chemical surface patterning provide a flexible platform for one-atom-thick 2D circuits with chemically/electrically modulated surfaces or lab-on-a-chip for bioapplications.

Supporting Information

Supporting Information is available from the Wiley Online Library or from the author.

Acknowledgements

A.M.v.d.Z., J.S., and S.P.K. were supported in part by an NSF-MRSEC under Award Number DMR-1720633 and the NSF-CAREER award under Award Number CMMI-1846732. D.S. and S.H. were supported by the Global Research and Development Center Program (2018K1A4A3A01064272), the Basic Science Research Program (2017R1A2B2010123), and the Priority Research Center Program (2010-0020207) through the National Research Foundation (NRF) of Korea. G.-H.L. acknowledges supports from the Basic Science Research Program, the Creative Materials Discovery Program, and the International Research & Development Program through the NRF of Korea (2016M3A7B4910940, 2018M3D1A1058794, and 2019K1A3A1A25000267). K.W. and T.T. acknowledge support from the Elemental Strategy Initiative conducted by the MEXT, Japan and the CREST (JPMJCR15F3), JST. This work was carried out in part in the Micro and Nano Technology Laboratory and the Materials Research Laboratory Central Facilities at the University of Illinois. The authors acknowledge helpful discussions with Jaehyung Yu, Mohammad Abir Hossein, Elif Ertekin, Nadya Mason, and Pinshane Huang.

Conflict of Interest

The authors declare no conflict of interest.

Keywords

2D compounds, fluorination, graphene, hydrogenation, patterned chemical functionalization

Received: May 29, 2019 Revised: July 19, 2019 Published online:

- G. Cheon, K. N. Duerloo, A. D. Sendek, C. Porter, Y. Chen, E. J. Reed, *Nano Lett.* **2017**, *17*, 1915.
- [2] L. M. Xie, Nanoscale 2015, 7, 18392.
- [3] X. Wang, G. Sun, P. Routh, D. H. Kim, W. Huang, P. Chen, Chem. Soc. Rev. 2014, 43, 7067.
- [4] D. Geng, N. Ding, T. S. A. Hor, Z. Liu, X. Sun, Y. Zong, J. Mater. Chem. A 2015, 3, 1795.
- [5] J. Xu, Y. Dou, Z. Wei, J. Ma, Y. Deng, Y. Li, H. Liu, S. Dou, Adv. Sci. 2017. 4. 1700146.
- [6] Q. Zeng, H. Wang, W. Fu, Y. Gong, W. Zhou, P. M. Ajayan, J. Lou, Z. Liu, Small 2015, 11, 1868.

- [7] L. Wang, P. Hu, Y. Long, Z. Liu, X. He, J. Mater. Chem. A 2017, 5, 22855.
- [8] D. Rhodes, D. A. Chenet, B. E. Janicek, C. Nyby, Y. Lin, W. Jin, D. Edelberg, E. Mannebach, N. Finney, A. Antony, T. Schiros, T. Klarr, A. Mazzoni, M. Chin, Y.-c. Chiu, W. Zheng, Q. R. Zhang, F. Ernst, J. I. Dadap, X. Tong, J. Ma, R. Lou, S. Wang, T. Qian, H. Ding, R. M. Osgood Jr., D. W. Paley, A. M. Lindenberg, P. Y. Huang, A. N. Pasupathy, M. Dubey, J. Hone, L. Balicas, Nano Lett. 2017, 17, 1616.
- [9] L. Zhao, M. Levendorf, S. Goncher, T. Schiros, L. Pálova, A. Zabet-Khosousi, K. T. Rim, C. Gutiérrez, D. Nordlund, C. Jaye, M. Hybersten, D. Reichman, G. W. Flynn, J. Park, A. N. Pasupathy, Nano Lett. 2013, 13, 4659.
- [10] S. P. Lonkar, Y. S. Deshmukh, A. A. Abdala, Nano Res. 2015, 8, 1039.
- [11] S. Lei, X. Wang, B. Li, J. Kang, Y. He, A. George, L. Ge, Y. Gong, P. Dong, Z. Jin, G. Brunetto, W. Chen, Z. T. Lin, R. Baines, D. S. Galvão, J. Lou, E. Barrera, K. Banerjee, R. Vajtai, P. Ajayan, Nat. Nanotechnol. 2016, 11, 465.
- [12] D. Pierucci, H. Henck, Z. B. Aziza, C. H. Naylor, A. Balan, J. E. Rault, M. G. Silly, Y. J. Dappe, F. Bertran, P. L. Fèvre, F. Sirotti, A. T. C. Johnson, A. Ouerghi, ACS Nano 2017, 11, 1755.
- [13] G. Bottari, M. A. Herranz, L. Wibmer, M. Volland, L. Rodríguez-Pérez, D. M. Guldi, A. Hirsch, N. Martín, F. D'Souza, T. Torres, Chem. Soc. Rev. 2017, 46, 4464.
- [14] J. T. Robinson, J. S. Burgess, C. E. Junkermeier, S. C. Badescu, T. L. Reinecke, F. K. Perkins, M. K. Zalalutdniov, J. W. Baldwin, J. C. Culbertson, P. E. Sheehan, E. S. Snow, *Nano Lett.* 2010, 10, 3001.
- [15] R. Stine, W. K. Lee, K. E. Whitener, J. T. Robinson, P. E. Sheehan, Nano Lett. 2013, 13, 4311.
- [16] J. Son, J. Kwon, S. P. Kim, Y. Lv, J. Yu, J. Y. Lee, H. Ryu, K. Watanabe, T. Taniguchi, R. Garrido-Menacho, N. Mason, E. Ertekin, P. Y. Huang, G. H. Lee, A. M. van der Zande, *Nat. Commun.* 2018, 9, 3988.
- [17] J. Son, S. Lee, S. J. Kim, B. C. Park, H. K. Lee, S. Kim, J. H. Kim, B. H. Hong, J. Hong, *Nat. Commun.* 2016, 7, 13261.
- [18] D. C. Elias, R. R. Nair, T. M. G. Mohiuddin, S. V. Morozov, P. Blake, M. P. Halsall, A. C. Ferrari, D. W. Boukhvalov, M. I. Katsnelson, A. K. Geim, K. S. Novoselov, *Science* 2009, 323, 610.
- [19] L. Zhang, J. Yu, M. Yang, Q. Xie, H. Peng, Z. Liu, Nat. Commun. 2013, 4, 1443.
- [20] I. Papadakis, Z. Bouza, S. Couris, A. B. Bourlinos, V. Mouselimis, A. Kouloumpis, D. Gournis, A. Bakandritsos, J. Ugolotti, R. Zboril, J. Phys. Chem. C 2017, 121, 22567.
- [21] I. Papadakis, Z. Bouza, S. Couris, V. Mouselimis, A. B. Bourlinos, J. Phys. Chem. C 2018, 122, 25573.
- [22] R. Balog, B. Jørgensen, L. Nilsson, M. Andersen, E. Rienks, M. Bianchi, M. Fanetti, E. Lægsgaard, A. Baraldi, S. Lizzit, Z. Sljivancanin, F. Besenbacher, B. Hammer, T. G. Pedersen, P. Hofmann, L. Hornekær, Nat. Mater. 2010, 9, 315.
- [23] M. Yi, W. Zhang, Z. Shen, X. Zhang, X. Zhao, Y. Zheng, S. Ma, J. Nanopart. Res. 2013, 15, 1811.
- [24] C. J. Russo, L. A. Passmore, Nat. Methods 2014, 11, 649.
- [25] W. Feng, P. Long, Y. Feng, Y. Li, Adv. Sci. 2016, 3, 1500413.
- [26] S. J. Nikkhah, M. R. Moghbeli, S. M. Hashemianzadeh, *Phys. Chem. Chem. Phys.* 2015, 17, 27414.
- [27] J. R. Felts, A. J. Oyer, S. C. Hernández, K. E. Whitener Jr., J. T. Robinson, S. G. Walton, P. E. Sheehan, *Nat. Commun.* 2015, 6, 6467.
- [28] H. Wang, F. Liu, W. Fu, Z. Fang, W. Zhou, Z. Liu, Nanoscale 2014, 6, 12250.
- [29] M. G. Stanford, P. D. Rack, D. Jariwala, npj 2D Mater. Appl. 2018, 2, 20.
- [30] J. Kang, D. Sarkar, Y. Khatami, K. Banerjee, Appl. Phys. Lett. 2013, 103, 083113.



ADVANCED MATERIALS

www.advmat.de

- [31] M. Medina-Sánchez, S. Miserere, A. Merkoçi, Lab Chip 2012, 12, 1932.
- [32] D. Wang, V. K. Kodali, W. D. Underwood II, J. E. Jarvholm, T. Okada, S. C. Jones, M. Rumi, Z. Dai, W. P. King, S. R. Marder, J. E. Curtis, E. Riedo, Adv. Funct. Mater. 2009, 19, 3696.
- [33] D. Haberer, C. E. Giusca, Y. Wang, H. Sachdev, A. V. Fedorov, M. Farjam, S. A. Jafari, D. V. Vyalikh, D. Usachov, X. Liu, U. Treske, M. Grobosch, O. Vilkov, V. K. Adamchuk, S. Irle, S. R. P. Silva, M. Knupfer, B. Büchner, A. Grüneis, Adv. Mater. 2011, 23, 4497.
- [34] Y. Li, Z. Chen, J. Phys. Chem. C 2012, 116, 4526.
- [35] R. Raj, S. C. Maroo, E. N. Wang, Nano Lett. 2013, 13, 1509.
- [36] F. Taherian, V. Marcon, N. F. A. van der Vegt, F. Leroy, *Langmuir* 2013, 29, 1457.
- [37] T. Lim, S. Ju, Surf. Coat. Technol. 2017, 328, 89.
- [38] J. Rafiee, X. Mi, H. Gullapalli, A. V. Thomas, F. Yavari, Y. Shi, P. M. Ajayan, N. A. Koratkar, *Nat. Mater.* 2012, 11, 217.

- [39] G. Zhao, X. Li, M. Huang, Z. Zhen, Y. Zhong, Q. Chen, X. Zhao, Y. He, R. Hu, T. Yang, R. Zhang, C. Li, J. Kong, J. B. Xu, R. S. Ruoff, H. Zhu, Chem. Soc. Rev. 2017, 46, 4417.
- [40] Y. J. Shin, Y. Wang, H. Huang, G. Kalon, A. T. S. Wee, Z. Shen, C. S. Bhatia, H. Yang, *Langmuir* 2010, 26, 3798.
- [41] Z. Xu, Z. Ao, D. Chu, A. Younis, C. M. Li, S. Li, Sci. Rep. 2015, 4, 6450.
- [42] J. H. Ko, S. Kwon, I. S. Byun, J. S. Choi, B. H. Park, Y. H. Kim, J. Y. Park, Tribol. Lett. 2013, 50, 137.
- [43] L. Wang, I. Meric, P. Y. Huang, Q. Gao, Y. Gao, H. Tran, T. Yaniguchi, K. Watanabe, L. M. Campos, D. A. Muller, J. Guo, P. Kim, J. Hone, K. L. Shepard, C. R. Dean, *Science* 2013, 342, 614.
- [44] F. Pizzocchero, L. Gammelgaard, B. S. Jessen, J. M. Caridad, L. Wang, J. Hone, P. Bøggild, T. J. Booth, *Nat. Commun.* 2016, 7, 11894